AIP | Applied Physics Letters

Strain induced effects on electronic structure of semi-metallic and semiconducting tin nanowires

Lida Ansari, Giorgos Fagas, and James C. Greer

Citation: Applied Physics Letters **105**, 123105 (2014); doi: 10.1063/1.4896293
View online: http://dx.doi.org/10.1063/1.4896293
View Table of Contents: http://scitation.aip.org/content/aip/journal/apl/105/12?ver=pdfcov
Published by the AIP Publishing

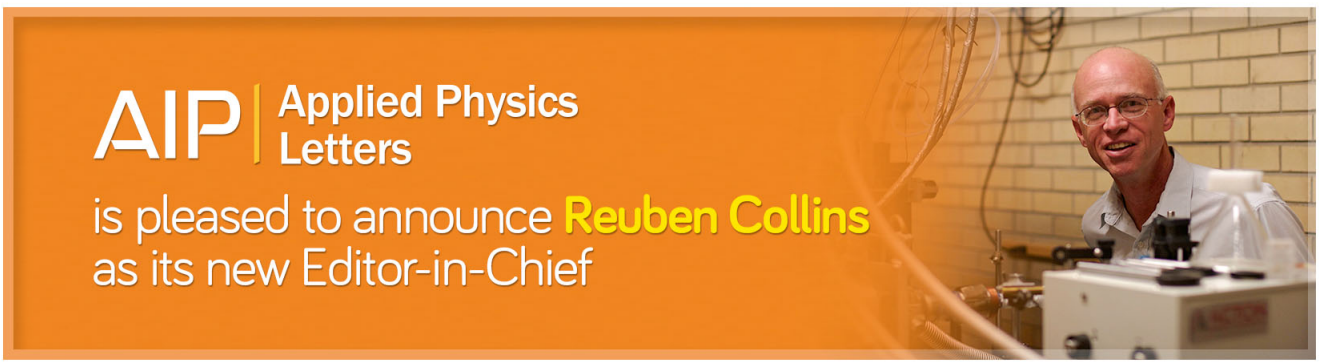

Strain induced effects on electronic structure of semi-metallic and semiconducting tin nanowires

Lida Ansari,[a] Giorgos Fagas, and James C. Greer
Tyndall National Institute, Dyke Parade, University College Cork, Cork, Ireland

(Received 8 July 2014; accepted 10 September 2014; published online 22 September 2014)

Semimetal nanowires are known to undergo a semimetal to semiconductor transition as a consequence of quantum confinement as their diameters are decreased. Using density functional theory calculations, the electronic structure of tin nanowires (SnNWs) under uniaxial strain within a range of −4% to +4% is investigated. It is demonstrated that a [110]-oriented semi-metallic SnNW with a diameter of ∼4.2 nm can be made either more metallic or semiconducting by the application of tensile or compressive strain, respectively. On the contrary, a [100]-oriented semi-metallic SnNW with a slightly larger diameter of ∼4.5 nm remains semiconducting with the application of either compressive or tensile strain. Carrier effective masses are calculated from the band structures; it is shown that for semimetal SnNW along [110] orientation the conduction and valence bands display near linear dispersion under both compressive and tensile strains (<3%) which leads to very small effective masses of $\sim 0.007 m_0$. We also show that strain energies and Young modulus vary with nanowire diameter and crystal orientation. The effect of alloying on the generation of tensile and compressive strains in SnNWs is also investigated. © *2014 AIP Publishing LLC*.
[http://dx.doi.org/10.1063/1.4896293]

Quasi-one dimensional nanostructures such as semiconductor nanowires are readily integrated into electronic systems. Nanoscale field effect transistors enable the continuation of Moore's law[1] in future technology generations through higher device density and consequently high function per unit area at lower unit cost. Critical to achieving this goal, the use of nanowire transistors permits efficient electrostatic control over the channel region allowing for ultra-low power nanoelectronics when used in multi-gate or gate-all-around configurations.

In order to continue the miniaturization of transistors below 10 nm critical dimensions, new device concepts and architectures are being introduced. Junctionless transistors, for example, do not require the formation of *p-n* junctions[2] and have been shown to be capable of operating at nanowires as small as 1 nm in diameter with a gate length of 3 nm.[3,4] Another new device concept being explored is the confinement modulated gap transistor (CMGT) where the limitations introduced by the requirement for introducing dopants in nanowires can be eliminated by exploiting the semimetal-to-semiconductor transition in sufficiently small diameter semimetal nanowires.[5] By thinning the central region in a semimetal nanowire, the conducting behavior of the wider semimetal regions is lost and a band gap is induced. This allows for the formation of Schottky barrier transistors in a single material by exploiting the quantum confinement in quasi-one-dimensional nanostructures.

The use of strain as a "technology booster" in transistor design is now a standard technique for modulating the electronic structure of Si to enhance both electron and hole mobilities.[6] In this study, the effect of uniaxial strain on the electronic structure of Sn nanowires (SnNWs) is investigated using density functional theory (DFT). It is demonstrated that strain can be applied in addition to geometry confinement to tune the bandgap and other electronic properties.

Nanowire atomic and electronic structures are determined by OpenMX (Open source package for Material eXplorer) based on Linear Combination of Atomic Orbitals (LCAO) representation of the Kohn-Sham orbitals and electron density.[7,8] The local-density approximation (LDA) is used for the exchange-correlation potential.[9] A numerical atomic orbital basis set for the tin atoms is defined using optimized orbitals with three orbitals per atomic level, or "triple-zeta" quality.[8] It is well known that the exchange correlation functional approximation in DFT introduces errors in band gap and lattice constants. Notwithstanding these limitations, the errors are well understood and DFT is a reliable means for predicting electronic and other material properties within acceptable errors allowing one to explore the physics behind the trends.

The atomic positions within all structures are relaxed starting from nanowires constructed from the α-tin phase by minimizing the total energy with respect to atomic coordinates until the maximum force component is less than 0.005 eV/Å. The simulation cell parameter along the nanowire axis is constrained during the optimization procedure to the value related to a chosen strain level. Transverse cell dimensions are chosen large enough to neglect the interaction between neighbouring nanowires arising from the periodic boundary conditions applied in the calculations. All nanowires have been passivated by hydrogen to eliminate any surface states and the calculations are performed at temperature 300 K. Uniaxial strain is introduced by modifying the unit cell along the nanowire axis. The coordinates of all atoms are relaxed after application of strain by elongating or reducing the cell parameter along the nanowire axis.

A cross-sectional view of the SnNW atomic structure for 2.8 nm diameter along [100] and 2.3 nm diameter along [110]

[a]Author to whom correspondence should be addressed. Electronic mail: Lida.Ansari@Tyndall.ie

is shown in Figs. 1(a) and 1(b), respectively. Fig. 1(c) shows the variation in the band gap energy with respect to tensile and compressive strain in [110]-oriented SnNWs with diameters $1.2\,\text{nm} \leq D_{NW} \leq 4.2\,\text{nm}$. Positive values refer to tensile strain, while negative values correspond to compressive strain. For smaller wire diameters a band gap is induced and wires are semiconducting, whereas larger wires (4.2 nm) are effectively semi-metallic.[10] As shown in Fig. 1(c), applying uniaxial compressive stain reduces the band gap of the semiconducting wires (i.e., 1.2 nm and 2.3 nm wire diameters) by up to 260 meV, while applying tensile strain leads to a small increase in their band gaps. For [100]-oriented SnNWs with diameters in the range of $1.3\,\text{nm} \leq D_{NW} \leq 4.5\,\text{nm}$, the nanowires are semiconducting and both tensile and compressive strains reduce the bandgap; see Fig. 1(d). The reduction under compressive strain is up to 134 meV for 1.3 nm- and 2.8 nm-diameter SnNW, and up to 218 meV reduction in the bandgap energy is obtained for 4.5 nm-diameter nanowire.

For the [110]-oriented SnNW with $D_{NW} = 4.2\,\text{nm}$, tensile strain modifies the nanowire electronic structure from semi-metallic to metallic character as is shown in Figs. 2(a) and 2(b). Also seen is that the off Γ valence valley increases in energy as tensile strain is applied leading to larger hole effective masses at the valence band edge as the band crossing occurs. As depicted in Fig. 2(c), DFT-LDA calculations predict a bandgap opening of ∼100 meV with application of 4% uniaxial compressive strain for the [110] orientation (recalling the typical underestimation of energy gaps in approximate DFT methods) causing a transition from semimetal to semiconductor characteristic. Therefore, it is demonstrated that it is possible to mechanically switch the electronic structure and consequently the charge transport behaviour from metallic to semiconducting by the application of strain.

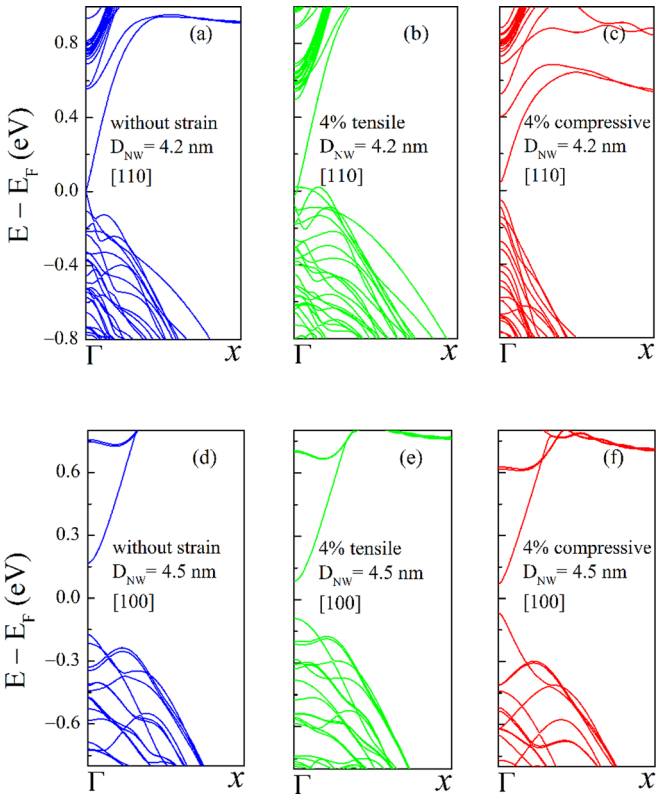

FIG. 2. Band structure of SnNW along [110] (a) without strain, (b) under tensile, and (c) under compressive strain. Applying compressive strain increases the band gap, while tensile strain enhances the metallic nature of the nanowire. Band structure of SnNW along [100] (d) without strain, (e) under tensile, and (f) under compressive strain. Energies are relative to the Fermi level.

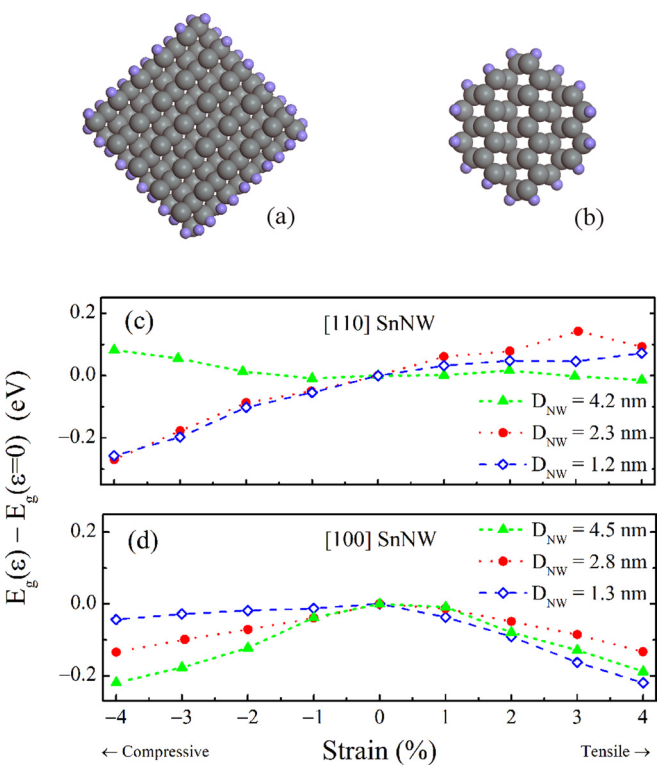

FIG. 1. Cross-section view of (a) 2.8 nm diameter [100] SnNW and (b) 2.3 nm diameter [110] SnNW. Bandgap energy variation with tensile and compressive strains for SnNW along (c) [110] and (d) [100].

The band structure of 4.5 nm-diameter SnNW along [100] orientation without strain and with tensile and compressive strains is plotted in Figs. 2(d)–2(f). The energies of conduction band edge are shifted towards lower energies and valence bands are moved towards higher energies under both tensile and compressive strain leading to a reduction in the band gap energies. Under compressive strain, as is shown in Fig. 2(f), the off Γ valence valley energy is lowered and therefore these valleys will contribute less to the hole transmission, and as a result higher carrier mobility is introduced.

Electron and hole effective masses are given as the curvature of the energy dispersion near valley minima. The electron and hole effective masses for different orientations and diameters as a function of strain are shown in Figs. 3(a) and 3(b). As can be seen, larger diameter nanowires possess smaller effective mass for both electrons and holes. The increase (by up to 150%) in hole effective mass for 4.5 nm [100] SnNW under tensile strain is due to the increase in the valence band valley curvature. Similar behaviour is observed for 2.8 nm [100] SnNW under >2% tensile strain; while the increase in the hole effective mass for the 2.3 nm [110] SnNW under >3% tensile strain is due to off Γ valence valley band crossing behaviour as shown in Fig. 3(c).

Fig. 3(d) shows a quasi-linear dispersion at the Γ valley for the conduction and valence bands for both relaxed and

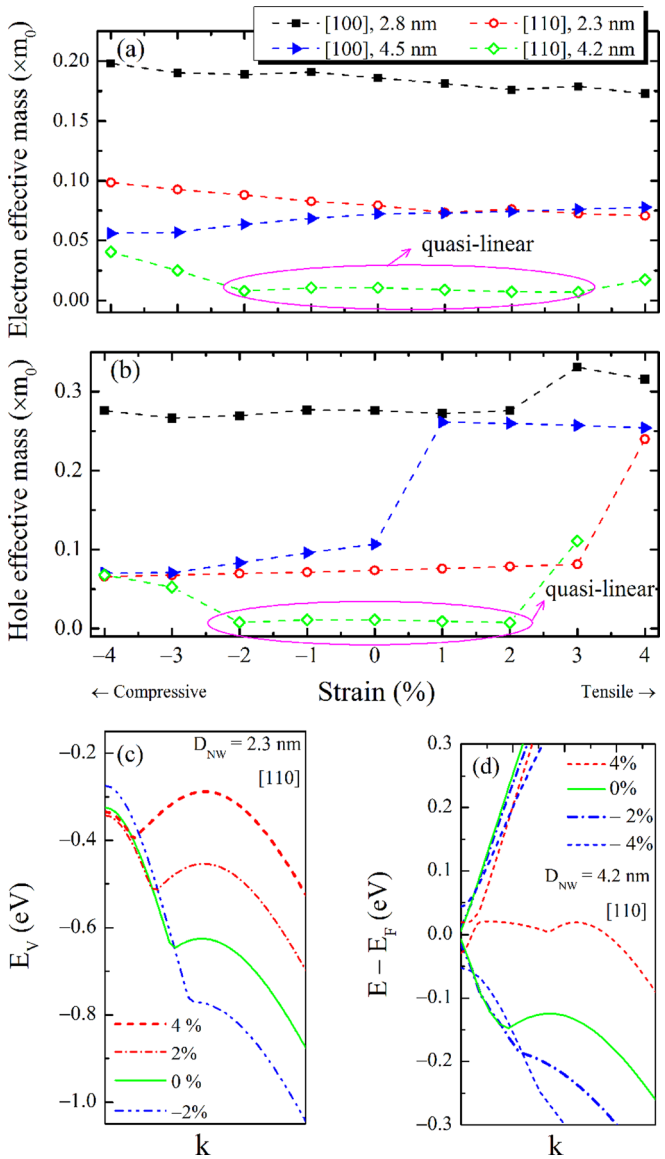

FIG. 3. Effective mass of (a) electrons and (b) holes with respect to strain for different crystallographic orientations and nanowire diameters. (c) Valence band profile for the 2.3 nm [110] SnNW under various strain conditions showing the off Γ valence valley band crossing behaviour. (d) Conduction and valence band edge profiles of [110] SnNW with 4.2 nm diameter under varying strain showing a quasi-linear dispersion.

for small strains in the 4.2 nm [110] SnNW. This results in a small effective mass of the order of $\sim 0.007 m_0$. For larger values of strain (>2%) the conduction band curvature becomes more parabolic, and the valence band off Γ valley band crossing leads to larger effective mass.

Young's modulus (Y), as a critical mechanical property of nanowires, has also been shown to depend on nanowire orientation and diameter.[11] Young's modulus is determined from[11]

$$Y = \frac{1}{V_0}\left(\frac{\partial^2 E}{\partial \varepsilon^2}\right)|_{\varepsilon=0},$$

where V_0 is the volume of relaxed nanowire, E is the strain energy, and ε is uniaxial strain.

The strain energy of SnNWs is plotted for tensile and compressive strains in Fig. 4. Young's modulus for the [110] and [100] SnNWs is calculated from the strain energy and is reported in Table I.

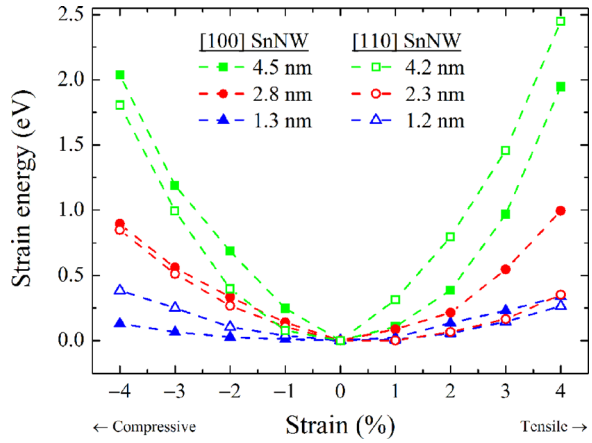

FIG. 4. SnNW strain energy with respect to tensile and compressive strains for the [110] and [100] orientations and different diameters. This reflects the Young's modulus.

For SnNWs, Young's modulus is larger for smaller diameters reflecting an increasing "stiffness". Nanowires oriented along [100] show smaller Young's moduli compared to [110]. For comparison, Young's modulus for bulk Sn is 41.4 GPa.[12]

A standard technique to introduce strain in nanoelectronics is the use of alloying in nanostructures. Strains in the range of 2%–4% have been realized for Si using Si_xGe_y alloys.[6] Sn_xGe_y alloys have also been synthesised for engineering the band structure of Ge.[13]

Here, we investigate inducing strain through alloying of a 2.3 nm-diameter SnNW along [110] orientation. As is shown in Fig. 5(a), by inserting 1.6% Ge substitutionally in the SnNW, a similar electronic structure as applying 2.5% compressive uniaxial strain is obtained. In other words, introducing 1.6% Ge into the nanowires modifies the unit cell length along the nanowire axis equivalent to applying 2.5% uniaxial strain. Under 3% tensile strain, as depicted in Fig. 5(b), the band gap energy reduction is lower comparing to alloying with Pb. Also, the off Γ valley responds differently between applying uniaxial strain and alloying with Pb. Similar behaviour is observed for nanowires oriented along the [100] direction.

In summary, we have studied the effect of uniaxial strain and strain effects associated with alloying in α-SnNWs. For specific orientations and diameters, uniaxial strain can be used to introduce a transition between metal to semimetal and semiconductor behaviour. This would allow controlling the electron transport properties through mechanical strain.

TABLE I. Young's modulus for SnNW along [100] and [110] orientations and different diameters.

[110]		[100]	
D_{NW} (nm)	Y (GPa)	D_{NW} (nm)	Y (GPa)
1.2	130.1	1.3	54.3
2.3	70.1	2.8	45.9
4.2	58.7	4.5	44.1

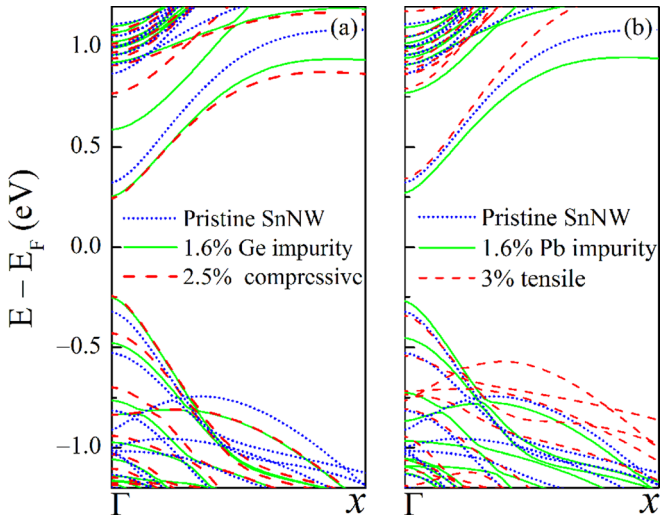

FIG. 5. Energy bands of (a) nanowire under compressive uniaxial strain as well as interstitial Ge impurity, and (b) nanowire under tensile uniaxial strain and interstitial Pb impurity in a 2.3 nm SnNW along [110]. Band diagram of pristine SnNW is also shown for comparison.

Carrier effective masses are calculated from the electronic structures; extremely reduced electron and hole effective mass ($\sim 0.007 m_0$) for small strain in [110]-oriented SnNWs with $D_{NW} \sim 4$ nm are found, due to a quasi-linear dispersion. It has been shown that Young's modulus of [100] orientation is smaller than [110] SnNW and for both orientations it increases with decreasing diameter. The effect of alloying on the generation of tensile and compressive strains in SnNWs is also investigated. Substitutional Ge shows similar effects on the band structure as compressive strain in pristine wires; consistent with Vegard's law. In contrast, Pd alloying behaves differently compared to uniaxial tensile stain.

This research was funded in part by the European Commission, through the 7th Framework Project SiNAPS (Contract No. 257856) and through a Science Foundation Ireland Principal Investigator award 13/IA/1956. The authors would like to acknowledge the SFI/HEA Irish Centre for High-End Computing (ICHEC) for the provision of computational facilities and support.

[1]G. E. Moore, Electronics **38**, 114 (1965).
[2]J.-P. Colinge, C.-W. Lee, A. Afzalian, N. D. Akhavan, R. Yan, I. Ferain, P. Razavi, B. O'Neill, A. Blake, M. White, A.-M. Keleher, B. McCarthy, and R. Murphy, Nat. Nanotechnol. **5**, 225 (2010).
[3]L. Ansari, B. Feldman, G. Fagas, J.-P. Colinge, and J. C. Greer, Appl. Phys. Lett. **97**, 062105 (2010).
[4]S. Migita, Y. Morita, M. Masahara, and H. Ota, J. Appl. Phys. **52**, 04CA01 (2013).
[5]L. Ansari, G. Fagas, J. P. Colinge, and J. C. Greer, Nano Lett. **12**, 2222 (2012).
[6]J. Bean, Science **230**, 127 (1985).
[7]T. Ozaki, Phys. Rev. B **67**, 155108 (2003).
[8]T. Ozaki and H. Kino, Phys. Rev. B **69**, 195113 (2004).
[9]J. P. Perdew and A. Zunger, Phys. Rev. B **23**, 5048 (1981).
[10]Bandgap energy of the SnNWs defined by DFT-LDA calculations is 2.3 eV and 0.34 eV for $D_{NW} = 1.3$ nm and 4.5 nm, respectively, for [100]-orientation; and 1.2 eV and 0.013 eV for $D_{NW} = 1.2$ nm and 4.2 nm, respectively, for [110]-orientation.
[11]B. Xu, A. J. Lu, B. C. Pan, and Q. X. Yu, Phys. Rev. B **71**, 125434 (2005).
[12]R. L. J. M. Ubachs, P. J. G. Schreurs, and M. G. D. Geers, IEEE Trans. Compon. Packag. Technol. **27**, 635 (2004).
[13]G. He and H. A. Atwater, Appl. Phys. Lett. **68**, 664 (1996).